



Oncogenic alterations reveal key strategies for precision oncology in melanoma treatment

Wei Sun^{1,2#}, Fang Zhao^{3#}, Tu Hu^{1,2#}, Zhiqiang Wu^{1,2#}, Yu Xu^{1,2}, Yan Dong^{1,2}, Biqiang Zheng^{1,2}, Chunmeng Wang^{1,2}, Wangjun Yan^{1,2}, Xiaoli Zhu^{2,4}, Jian Wu⁵, Michael J. McKay⁶, Imanol Arozarena⁷, Lluçia Alos⁸, Cristina Teixeira⁸, Yong Chen^{1,2}

¹Department of Musculoskeletal Oncology, Fudan University Shanghai Cancer Center, Shanghai, China; ²Department of Oncology, Shanghai Medical College, Fudan University, Shanghai, China; ³Department of Dermatology, University Hospital Essen, Essen, Germany; ⁴Department of Pathology, Fudan University Shanghai Cancer Center, Shanghai, China; ⁵MyGenostics Inc., Beijing, China; ⁶Department of Radiation Oncology, Northern Cancer Service, Burnie, Australia; ⁷Navarrabiomed-Fundación Miguel Servet-Idisna, Complejo Hospitalario de Navarra, Pamplona, Spain; ⁸Department of Pathology, Hospital Clinic of Barcelona, Barcelona, Spain

Contributions: (I) Conception and design: W Sun, F Zhao, Z Wu, T Hu, Y Chen; (II) Administrative support: MJ McKay, I Arozarena, L Alos, C Teixeira, Y Chen; (III) Provision of study materials or patients: Y Dong, B Zheng, C Wang, W Yan, X Zhu; (IV) Collection and assembly of data: W Sun, J Wu; (V) Data analysis and interpretation: W Sun, F Zhao, T Hu, Z Wu; (VI) Manuscript writing: All authors; (VII) Final approval of manuscript: All authors.

#These authors contributed equally to this work.

Correspondence to: Yong Chen. Department of Musculoskeletal Oncology, Fudan University Shanghai Cancer Center, No. 270, Dongan Road, Shanghai 200032, China. Email: cheniyong@fudan.edu.cn.

Background: Molecular profiling with next-generation sequencing (NGS) has been applied in multiple solid tumors, including melanomas, to identify potential drug targets. However, the association between clinical outcomes and the molecular alterations has not yet been fully clarified.

Methods: A total of 108 patients with melanoma were included in this study, 95 of whom had both sequencing data and clinical outcomes were collected. We analyzed the genetic alterations of 108 malignant melanoma patients using the OncoCare panel, which covers 559 genes.

Results: A model was also established to predict side effects through a combination analysis of clinical data and somatic variants, yielding an area under the receiver operating characteristic curve (AUROC) score of 0.8. We also identified epidermal growth factor receptor (EGFR) mutation was excellent predictor for progression-free survival (PFS) for patient who received immunotherapy (log-rank P=0.01), while tumor mutation burden (TMB) was found to not be significantly associated with PFS (log-rank P=0.87). Combining clinical features with genetic analysis, we found that patients carrying both DNA POLD1/ALOX12B or POLD1/PTPRT mutations had a significantly lower survival rate.

Conclusions: Overall, these results demonstrate the benefits of applying NGS clinical panels and shed light on future directions of personalized therapeutics for the treatment of melanoma.

Keywords: Melanoma; genetic alterations; next-generation sequencing panels (NGS panels); machine learning; prognostic predictors

Submitted Oct 27, 2022. Accepted for publication Nov 18, 2022.

doi: 10.21037/atm-22-5346

View this article at: <https://dx.doi.org/10.21037/atm-22-5346>

Introduction

Malignant melanoma is the most lethal form of skin cancer and is extremely aggressive and difficult to cure due to its high metastatic potential. The 5-year survival rate of patients with metastatic malignant melanoma is approximately 5–19%, with an estimated median survival of 5.3 months (1). The American Cancer Society estimated 100,350 new cases of skin melanoma and 6,850 related deaths in 2020 (2); therefore this disease constitutes a heavy burden on the medical system and society. The mortality of melanoma has declined in recent years, probably due to the application of newly approved drugs (3). However, in many cases, these promising therapies appear to lose their healing effect. These failures emphasize the importance and urgency of developing and applying precision oncology.

Recent years have witnessed the emergence of targeted therapies for malignant melanoma, and the combination of a *BRAF* inhibitor with a MEK inhibitor has become the standard regimen for *BRAF*^{V600} mutation-positive melanoma (4). Although the median progression-free survival (PFS) has increased to 11–14.9 months with combination therapy and the disease control rate has exceeded 90%, complete responses have only been observed in 16% of the patients (5,6). Checkpoint blockade therapeutics have also shown superior efficacy in the treatment of advanced melanoma, prolonging the median survival to 19.3–35.8 months compared to 8.1–13.7 months in patients receiving chemotherapy (7–10). Nevertheless, primary and

secondary resistance to programmed cell death protein 1 (PD-1) checkpoint inhibition was reported to reach 60% and 20–30%, respectively (4). Regarding the c-Kit targeting tyrosine kinase inhibitor, the response rate was indicated to be low to 23–26%, while stable disease was found in only 30–46% of patients with *KIT* mutation (11,12). The relatively low response rate and high resistance rate have been attributed to a failure to identify the most suitable patients for this type of therapy.

To understand the clinical features and prognostic implications of malignant melanoma, the key alterations of the target genes need to be identified, and the overall mutation landscape and genomic profiles need to be clarified (13). Next-generation sequencing (NGS) technologies have matured and have been developed in multiple validated pipelines, aiding in effectively identifying various target alterations and enabling timely and cost-effective genetic testing (14). Therefore, NGS-based platforms confer substantive advantages in the application of therapeutic strategies and the practice of precision oncology.

Various NGS-based panels have been established and described to study the etiology and prognosis of melanoma. For instance, Park *et al.* applied an NGS panel in Korean patients with malignant melanoma to detect single-nucleotide variants (SNVs), small insertions/deletions, copy number variations (CNVs), and structural variations to estimate tumor mutation burden (TMB) (15). Seventy percent of the enrolled patients were found to have actionable alterations, while the TMB was associated with PFS (15). NGS-based technologies have also been used to screen for those patients suitable for certain therapies. Johnson *et al.* performed hybrid capture-based NGS on American patients (16). Compared with the intermediate and low mutational load groups, patients with higher mutational loads were found to have a superior response rate to anti-programmed death-ligand 1 (PD-L1) therapy, PFS, and overall survival (OS) (16). Using NGS, Conroy *et al.* demonstrated that, in American patients classified with high PD-L1 expression, the overall response rate was 2–5 folds higher than the patients with low PD-L1 expression (17). In another study, Lokhandwala *et al.* used an NGS-based panel to categorize the range, frequency, and coexisting driver mutations of the different classes of *BRAF* mutations in an American cohort. They found that the panel used was valuable for elucidating the clinical outcome and benefits of *BRAF*-targeted therapy (18). However, few NGS panel studies have focused on the Chinese population, which, when the distinct genetic background of

Highlight box

Key findings

- A NGS panel-based combination analysis of clinical data and somatic variants predicts clinical outcomes with prominent performance.

What is known and what is new?

- Molecular profiling with NGS has been applied in melanomas. However, the association between clinical outcomes and the molecular alterations is not well understood.
- Machine learning model was established to predict side effects through a combination analysis of clinical data and somatic variants. *EGFR* mutation was an excellent predictor for PFS for patients who received immunotherapy.

What is the implication, and what should change now?

- Our study demonstrates the benefits of applying NGS clinical panels and shed light on future directions of personalized therapeutics for the treatment of melanoma.

this population is considered, may yield diverse mutation features arising from the variety of ethnic groups. Finally, very little is known about the linkage between different genetic alterations and potential clinical outcomes, such as response to different therapeutics and potential side effects.

This situation prompted us to investigate the association of clinical features and genetic landscape using a comprehensive NGS panel in a series of 108 Chinese melanoma patients.

Methods

Patients and samples

From March 2018 to June 2019, we consecutively selected a total of 108 patients with pathologically diagnostic melanoma from Fudan University Shanghai Cancer Center (FUSCC).

The clinical data and biochemical profiles were obtained from patients' medical records. Pathological stage were defined according to the 8th edition of the American Joint Committee on Cancer (AJCC) cancer staging manual (19). Patients were followed up until death or June 30, 2020. Disease-free survival (DFS) was defined as the time interval from radical surgery to local recurrence or distant metastasis. Recurrence or metastasis was confirmed by pathology or imaging follow-up. Adverse side effect was graded according to Common Terminology Criteria for Adverse Events (version 4.03).

The study was conducted in accordance with the Declaration of Helsinki (as revised in 2013). This study was approved by the Medical Ethics Committee of FUSCC (No. 1903198-8) and informed consent was taken from all the patients.

Immunohistochemistry (IHC)

IHC was performed by the department of pathology, FUSCC. To be brief, immunostaining was performed by using an automated BenchMark XT staining system (Ventana Medical Systems, Tucson, AZ, USA) according to manufacturer's instructions. Proteins were detected using the following antibodies: p16 (1:100, Ventana), AE1/AE3 (1:50, Dako), Ki-67(1:150, Dako), Melan-A (1:50; Dako), HMB45 (1:50, Dako), PNL2 (1:100; MXB Biotechnologies), S-100 (1:700; Dako), SOX10 (1:200; Gene Tech), BRAF (1:50, VE1, Ventana). The antibodies that were chosen to annotate melanoma were recommended from National

Comprehensive Cancer Network (NCCN) melanoma guidelines. 3,3'-diaminobenzidine tetrahydrochloride (DAB) was applied to detect the presence of each biomarker in the clinical samples. Finally, the slides were counterstained with hematoxylin for nucleic staining.

DNA isolation and sequencing

Genomic DNA was extracted from fresh-frozen tumor samples and their paired peripheral blood respectively. Briefly, the column extraction method was used for tissue and magnetic bead extraction method was used for blood, according to their instructions respectively (MyGenosites Inc., Beijing, China). The extracted DNA of 3 µg was fragmented to an average size of 180 bp using a Bioruptor sonicator (Diagenode, Belgium), which was used to generate the index libraries (average size of 350–450 bp, with adapter) using the Library Preparation Kit (MyGenosites Inc.), according to the requirements of Illumina platform. Target enrichment experiment was performed following the standard protocol of the GenCap Kits (MyGenosites Inc.). The enrichment libraries were sequenced on Illumina HiSeq X ten sequencer for paired reading of 150 bp. The mean sequencing depth was 1,000×, with variant accuracy >99%.

A target sequencing panel named OncoCare (designed by MyGenosites Inc.) was implemented in this study. The panel included 559 tumor-related genes, which were most frequently reported genes involved in carcinogenesis and tumor development (Table S1).

Genomic DNA was extracted from tumor samples and their paired peripheral blood respectively. The extracted DNA was fragmented to an average size of 180 bp using a Bioruptor sonicator (Diagenode), which was used to generate the index libraries (average size of 350–450 bp, with adapter) using the Library Preparation Kit (MyGenosites Inc.), according to the requirements of Illumina platform. Target enrichment experiment was performed following the standard protocol of the GenCap Kits (MyGenosites Inc.). The enrichment libraries were sequenced on Illumina HiSeq X ten sequencer for paired reading of 150 bp.

Sequencing data analysis

Somatic mutation and CNV data were analyzed. For mutation, we selected those with sequencing depth of no less than 20 and alternative reads of no less than 5. We also removed reads that may potentially be false positive

Table 1 Patient demographics (n=108)

| Demographics | N (%) |
|----------------------|-----------|
| Age (years) | |
| 0–30 | 4 (3.7) |
| 30–60 | 50 (46.3) |
| 60–90 | 54 (50.0) |
| Gender | |
| Male | 51 (47.2) |
| Female | 57 (52.8) |
| Primary lesion type | |
| Acral | 57 (52.8) |
| Cutaneous | 28 (25.9) |
| Mucosal | 14 (13.0) |
| Unknown | 9 (8.3) |
| Stage | |
| IIA | 7 (6.5) |
| IIB | 29 (26.9) |
| IIC | 12 (11.1) |
| IIIB | 5 (4.6) |
| IIIC | 51 (47.2) |
| IIID | 4 (3.7) |
| Adverse effect level | |
| <3 | 91 (84.2) |
| 3 | 17 (15.8) |

with mapping quality (MAPQ) less than 20 or secondary alignment. For CNV, we selected those with absolute value of log₂ ratio larger than 2 which is equivalent to a copy number of larger than 4 or smaller than 1. For somatic mutation, only nonsynonymous SNVs, insertions, deletions, and splice site mutations were analyzed. TMB was defined as the number of somatic mutations, including all base substitutions, insertions, and deletions, per megabase of analyzed genome. Calculations were performed according to the method described by Chalmers (20). Specifically, considering that the frequent synonymous variants may indicate nonsynonymous changes, we counted synonymous mutations to reduce sample noise. As the targeted sequencing panel is biased towards genes that typically mutate in cancer patients, somatic mutations in

the Catalogue of Somatic Mutations in Cancer (COSMIC) region were not counted. The resulting number of somatic mutations was divided by the size of the coding region to obtain the TMB per megabase.

Statistical analysis

Permutation importance scores were used to evaluate feature importance. Each evaluation score was averaged over 100 repeated runs. Statistical models including random forest classifier, gradient boost classifier, XGBoost classifier, and Naïve Bayes were considered. We used a genetic algorithm (Tree-Based Pipeline Optimization Tool) to select the best model and optimize its hyperparameters. The area under the receiver operating characteristic curve (AUROC) score, was used to evaluate model accuracy. We also calculated other metrics for comparison purposes. All models were trained and validated using a 5-fold cross validation with stratified train-test splits that preserve the percentage of samples for each prediction target. All metrics were averaged over 20 repeated runs. For classification of significantly imbalanced target (ratio between two classes is larger than 2), we up-sampled the minor class to match the size of major class. All statistical models were trained and validated using scikit-learn. All statistical tests including log-rank test and chi-square test were performed using the stats package in Python.

Results

Clinical features and outcomes

A total of 108 patients with melanoma were included in the study, 95 of whom had both sequencing data and clinical outcomes were collected. Patient demographics are shown in *Table 1*. The median age of the patients was 59.5, and 57 (52.8%) patients were female. The dominant primary lesion type was acral (57/95; 52.8%), cutaneous and mucosal melanoma accounted for 25.9% and 13.0%, respectively. 44.5% of patients were at stage II while others were at stage III. While most patients showed mild adverse effect with adverse effect level of less than 3, 15.8% of them showed level 3 adverse effect.

The IHC results revealed a panel of 9 markers (*Figure 1A*, *Figure S1*). As IHC results were missing for 10 patients, only markers that were identified in more than 10 patients were shown to represent the top markers. Most patients (79.6%) were characterized with more than 1 marker.

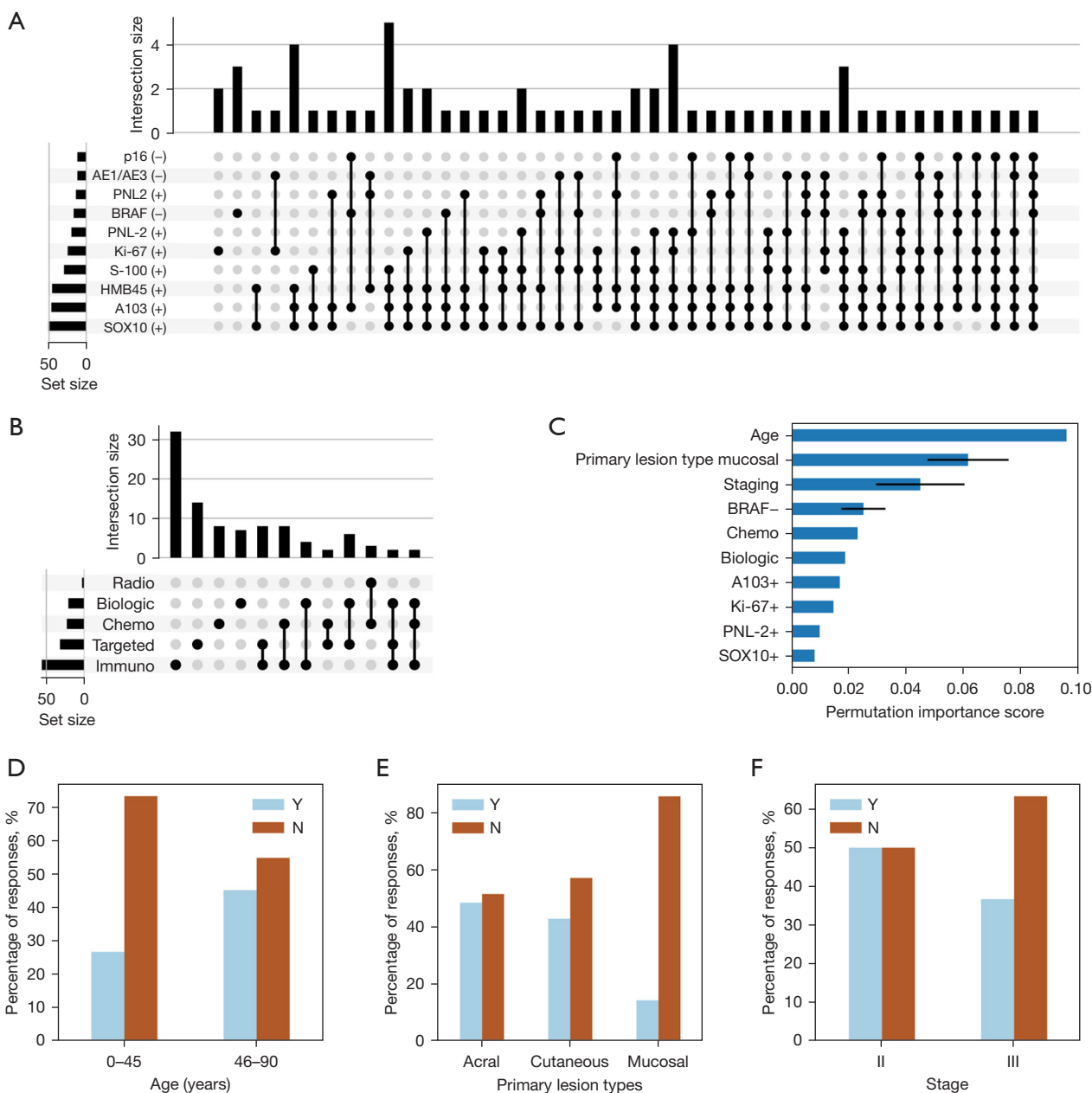


Figure 1 Clinical data and their relation to response. (A) IHC results for all patients. Only markers that were identified in more than 10 patients are shown to represent the top markers. Co-occurring markers were presented by the intersections. (B) Combinatorial treatment types for all patients. Co-occurring treatment types were presented by the intersections. (C) Permutation importance score for top clinical features that were related to clinical outcome. (D-F) Percentages of responses in the top 3 features. Y, response (yes); N, no response; IHC, immunohistochemistry.

The patients received five different types of treatment, including radiotherapy (2.8%), biologic treatment (19.4%), chemotherapy (21.3%), targeted therapy (29.6%), and immunotherapy (51.9%). A number of patients (43.5%) also received treatment combinations (Figure 1B). We considered

a random forest model to relate different clinical features with treatment response and used a permutation importance score to rank the features (Figure 1C). Age and stage were among the dominant features that were related to response. Lesion type, especially mucosal, was also a top feature due

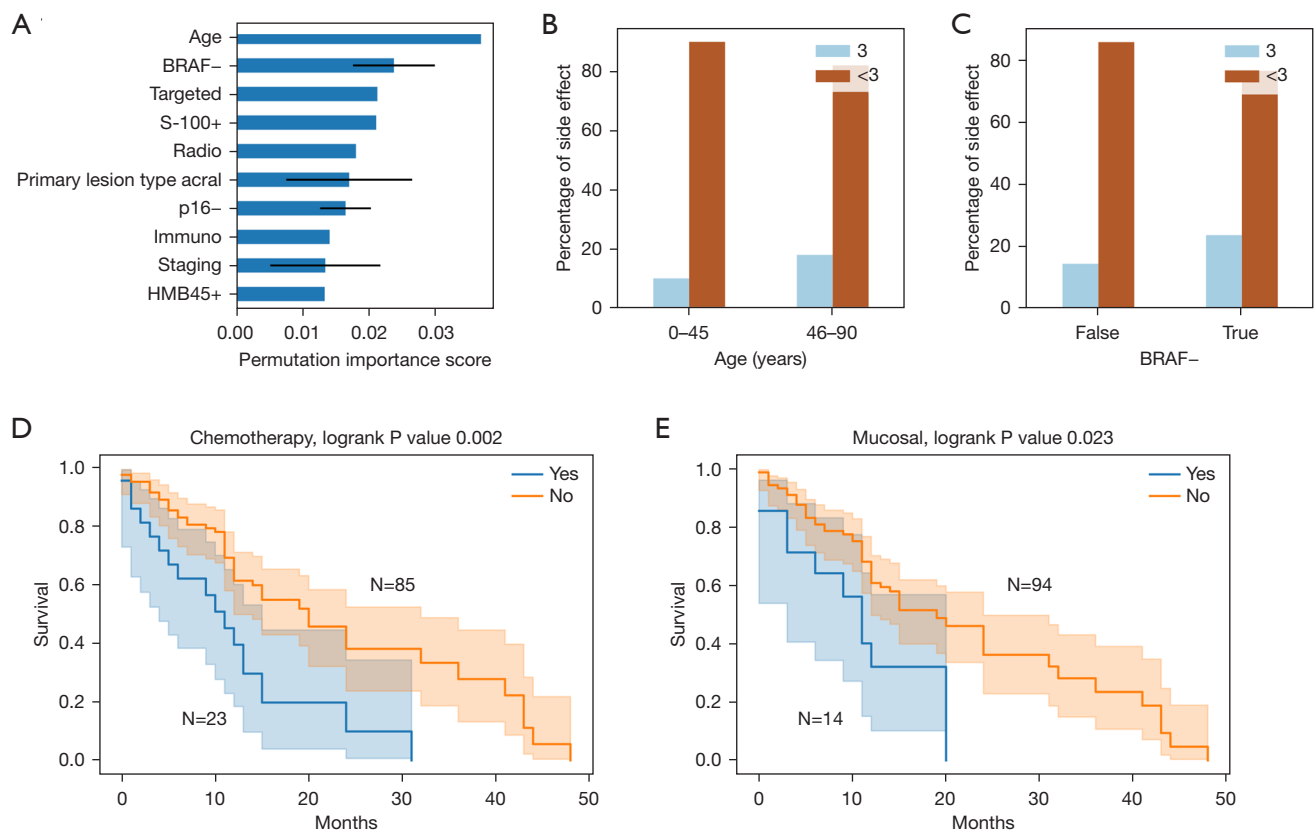


Figure 2 Relationship of clinical features with side effects and PFS. (A) Permutation importance score for most significant clinical features that were related to side effects. (B,C) Percentages of side effect numbers in the top 2 features. (D,E) Kaplan-Meier plots revealing the relationship of chemotherapy and mucosal lesion type with PFS. PFS, progression-free survival.

to its relationship with stage. Most mucosal lesions were in stage III (10 in stage III *vs.* 4 in stage II), while other lesion types were almost evenly distributed between two stages (28 in stage III *vs.* 29 in stage II for acral and 13 in stage III *vs.* 15 in stage II for cutaneous). Although other features including *BRAF*(-), chemotherapy, and biologic therapy contributed to the relation, they were not as significant as age, stage, or lesion type, whose detailed relations to response were further analyzed. First, younger patients showed worse treatment response (chi-square $P=2\times 10^{-4}$, *Figure 1D*). This was shown by the comparison between the below 45-year-old group (21 patients) and the above 45-year-old group (87 patients, at 45 chi-square P value was optimized). Second, mucosal melanoma exhibited the worst response to treatment (chi-square $P=2\times 10^{-4}$, *Figure 1E*). Third, melanoma with more advanced stages showed worse response to treatment (chi-square $P=1\times 10^{-4}$, *Figure 1F*).

In addition to treatment response, we also analyzed the relation of the clinical features to PFS and side effects,

with the same analysis being applied to side effects. The relationship of clinical features to side effects was not as significant as that to treatment response as indicated by the permutation importance score (*Figure 2A*). The most significant identified features, age and *BRAF*(-), showed much less difference among the feature levels as opposed to those in response (chi-square $P=0.44$ and 0.03 , *Figure 2B,2C*, respectively). Two other features, chemotherapy and mucosal lesion type, were also identified as being significantly related to PFS, with their log-rank $P<0.05$ (*Figure 2D,2E*). Specifically, patients who received chemotherapy or patients with mucosal melanoma showed a significantly worse survival rate (log-rank $P=0.002$ and 0.023 , respectively).

Oncogenic alterations

The sequencing data were analyzed with the genetic alteration patterns being summarized in *Figure 3*. SNV

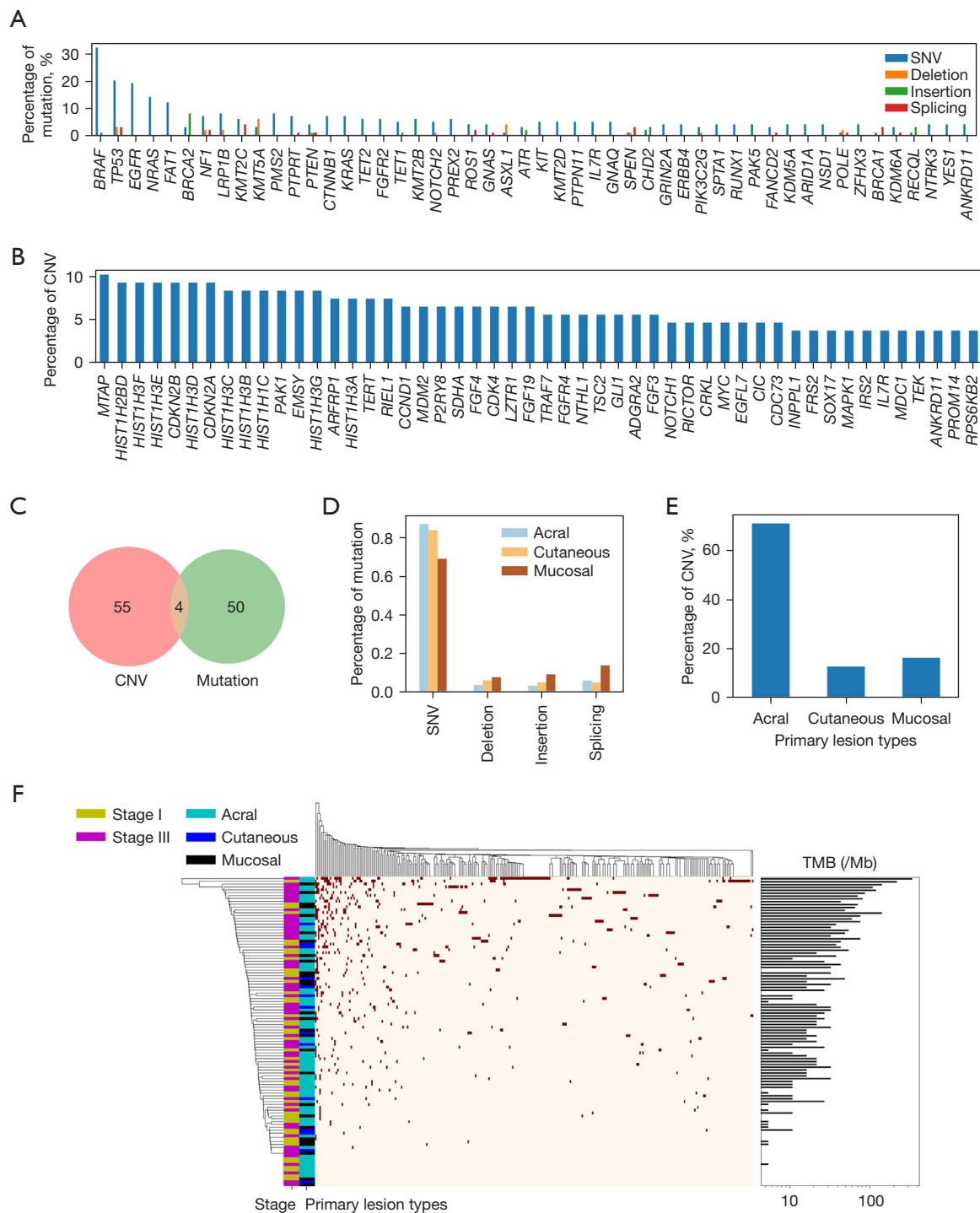


Figure 3 Oncogenic alteration features. (A,B) Percentages of (A) mutation and (B) CNV of genes with a top 50 frequency of occurrence across patients. (C) Venn diagram of the genes with frequent mutations and CNV. (D,E) Percentages of (D) mutation and (E) CNV for all primary lesion types. (F) Oncogenic alteration statistics and TMB for all patients. The row color panels correspond to the stage and primary lesion type, respectively. SNV, single-nucleotide variant; CNV, copy number variation; TMB, tumor mutation burden.

was the dominant mutation type across most of examined genes. More than 30% of the patients harbored the *BRAF* mutation and there were 7 genes with mutation harbored by more than 10% of the patients (Figure 3A). The frequency of CNV was in general less than mutation and *MTAP* is the only gene with significant CNV in more than 10% of the patients (Figure 3B). We compared frequent mutations and CNVs (both identified by K-means clustering of two clusters) across all patients and found that they have only 4 overlapped in gene symbols (Figure 3C). We then analyzed the distribution of different types of mutations and CNVs among different primary lesion types. The distribution of mutation type was almost consistent across different primary lesion types with mucosal lesion slightly in favor of splicing (Figure 3D). Most CNV (71%) occurs with patients with acral melanoma (Figure 3E). The frequencies of oncogenic alterations (either mutation or CNV in a gene) for each patient were analyzed along with TMB (Figure 3F). Stage III patients harbored significantly more oncogenic alterations than stage II patients (Mann-Whitney U-test $P=0.02$). No significant difference was found among different lesion types (Kruskal-Wallis H-test $P=0.77$). Additionally, no significant difference of TMB was found among either stages or lesion types (Mann-Whitney U-test $P=0.24$ and Kruskal-Wallis H-test $P=0.86$, respectively).

Molecular features as predictors for clinical outcome

Oncogenic alterations were highly associated with clinical outcome for the patients in the cohort. We first identified 4 hotspot mutations in 4 genes including *BRAF*, *BRCA2*, *KMT5A*, and *NRAS*. Here hotspot mutation is defined as mutation location that occurs in more than 5% of the patient. We then evaluated the relationship of all genetic mutations and CNVs with PFS and found that *NF1* mutation, *TET2* mutation, and *BRCA2* mutation were significantly related to patient PFS (log-rank $P=0.01$, 0.02 , and 0.04 , respectively). When the combination of genetic mutations was considered, more significant associations could be observed. For example, *NF1*- or *BRCA2*-mutated, and *EGFR*- or *TP53*-mutated patients had the worst PFS rate (log-rank $P=0.006$ and 0.012 in Figure 4A,4B, respectively). If molecular and clinical features were both considered, the top differentiators for PFS from the combined feature set are patients with *NF1* mutation or receiving chemotherapy and patients with *NF1* mutation or with mucosal melanoma (log-rank $P=0.0001$ and 0.0004 in Figure 4C,4D, respectively).

Oncogenic alterations were excellent predictors for treatment response, but the prediction accuracy was better than that of clinical features alone (Figure 4E). We used permutation importance to rank the features and genetic algorithms for optimizing the models for both feature sets: clinical and molecular (sequencing), and clinical only. The optimized model, a gradient boosting classifier, was the same for both feature sets. Nevertheless, the optimized hyperparameters differed for the 2 feature sets. The optimal number of features to be included in the models was also different between the 2 feature sets: 12 features were included for clinical and molecular features and 8 features were included for clinical features only. Among the optimized 12 features for clinical and all molecular features, age, mucosal lesion, acral lesion, *A103(+)*, *SOX10(+)* were the clinical feature included. The molecular features included *SDHA* CNV, *CDKN2B* CNV, *CDKN2A* CNV, *FAT1* mutation, *CTNNB1* mutation, *TERT* CNV, *FGFR4* CNV. Adding oncogenic alterations yielded an AUROC score of 0.8 which was improved from the 0.60 from using clinical features alone.

Adding oncogenic alterations significantly improve the predictability for the adverse effect level, with the AUROC score increasing from 0.55 to 0.73 (Figure 4F). For these 2 models, the gradient boosting classifier was the optimized model for clinical and molecular features, and the k-nearest neighbor classifier was the optimized model for the clinical feature only model. The optimal numbers of features included in the models were 20 for clinical and molecular features and 15 for clinical features only. The 20 selected features for the clinical and molecular feature set were age, *SDHA* CNV, *CDKN2B* CNV, *TERT* CNV, *FGFR4* CNV, *CDKN2A* CNV, radiotherapy, mucosal lesion, *FAT1* mutation, immunotherapy, *NTHL1* CNV, *PNL2(+)*, *PTEN* mutation, *MTAP* CNV, targeted therapy, biologic therapy, staging, *SOX10(+)*, chemotherapy, and *BRCA2* mutation. Other evaluation metrics for the optimized models are shown in Table 2. There were in total 5 features that are significantly related to PFS, including *NF1* mutation, *TET2* mutation, and *BRCA2* mutation, chemotherapy and mucosal lesion. In contrast, the important features for PFS and patient response had zero overlap (Figure 4G).

The analysis of both clinical and molecular features can also shed light on directions for personalized therapeutics. To confirm the effect of the oncogenic alterations on clinical outcomes of different treatment types, we then selected the 56 patients who have received immunotherapy. It is believed that TMB is associated with clinical outcome, especially survival for different cancers after immunotherapy (15,21).

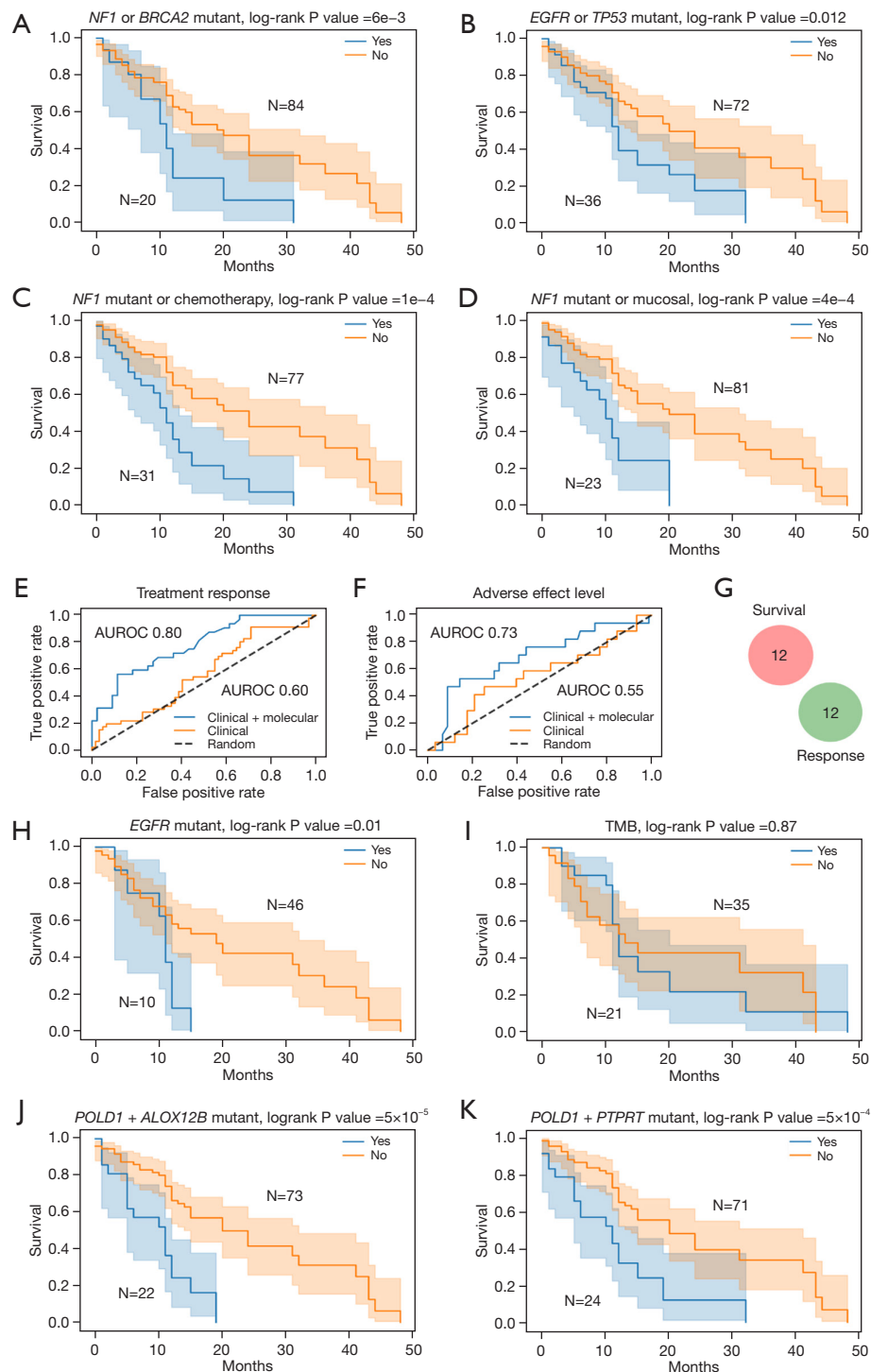


Figure 4 Relationship of sequencing features with clinical outcome. (A,B) Top differentiators from molecular features for PFS. (C,D) Top differentiators from both molecular and clinical features for PFS. (E,F) ROC of prediction models for treatment response and side effect level. (G) Venn diagram showing the relationship between the selected features for survival and patient response. (H,I) Top differentiator and TMB for PFS for patients receiving immunotherapy (J,K) Kaplan-Meier plots for mutated DNA *POLD1* + *ALOX12B* and mutated *POLD1* + *PTPRT*. AUROC, area under the receiver operating characteristic curve; TMB, tumor mutation burden; PFS, progression-free survival; ROC, receiver operating characteristic.

Table 2 All metrics for the predictive models for treatment response and level of side effects

| Features | Response | | Side effect | |
|-------------|-------------|----------------|-------------|----------------|
| | Clinical | Clinical + NGS | Clinical | Clinical + NGS |
| Precision | 0.56 (0.08) | 0.68 (0.12) | 0.50 (0.07) | 0.59 (0.09) |
| Recall | 0.55 (0.10) | 0.67 (0.06) | 0.47 (0.07) | 0.64 (0.14) |
| AUROC score | 0.60 (0.10) | 0.80 (0.11) | 0.55 (0.13) | 0.73 (0.16) |
| F1 score | 0.54 (0.08) | 0.65 (0.07) | 0.49 (0.06) | 0.57 (0.12) |
| Accuracy | 0.56 (0.08) | 0.72 (0.08) | 0.74 (0.07) | 0.66 (0.13) |

The numbers in parentheses are standard deviations of the five validation splits. NGS, next-generation sequencing; AUROC, area under the receiver operating characteristic curve.

Here, we identified EGFR mutation was excellent predictor for PFS for patient who received immunotherapy (log-rank $P=0.01$), while TMB was found to not be significantly associated with PFS (log-rank $P=0.87$) (Figure 4H,4I). In addition, *POLE* and *POLD1* mutations have been reported as biomarkers for immunotherapy outcomes for multiple cancer types including melanoma (22). We identified that patients who had combination mutations of *POLD1/ALOX12B* and *POLD1/PTPRT* had the worst PFS rate (Figure 4J,4K). In summary these results presented benefits of applying NGS clinical panels for personalized therapeutics for the treatment of melanoma.

Discussion

In this study, we analyzed 108 patients' genetic alterations across SNVs, CNVs, insertion-deletions, and estimated TMBs in the patients using the commercial OncoCare panel. Compared to the previous study (15), our study includes a larger sample size (108 *vs.* 36) with a more detailed patient information collection, such as treatment types, treatment responses, and side effect levels. We identified that patients who had combination mutations of *POLD1/ALOX12B* and *POLD1/PTPRT* had the worst PFS rate. We also proved that the usage of NGS panel could be a much better solution to predicting the treatment response with an AUROC score of 0.8 as compared to using the clinical data alone. Moreover, we also established a powerful model for predicting the side effects for the patients, with the combination analysis of the clinical data and the molecular alterations, yielding an AUROC score of 0.73. Finally, our data also provided insights into precision oncology as we identified *EGFR* mutation was excellent predictor for PFS for patient who received immunotherapy.

Acral melanoma patients accounted for 52.8% of all Asian melanoma patients. Previous studies demonstrated the poor response of acral melanomas to immune checkpoint inhibitors (23,24). This may be due to low *PD-L1* expression in the tumor microenvironment and low numbers of tumor-infiltrating lymphocytes (TILs) (23,24). Targeted therapies with inhibitors like imatinib to acral melanoma also result in poor and non-durable responses (12). Therefore, chemotherapy still plays an important role in the treatment, especially in posterior lines, of acral melanoma. Hence, these results may be useful in the precise treatment of acral melanoma.

Overall, these results suggest that clinical application of NGS panel screen will be a strong tool for not only discovering various types of genetic alterations, but also predicting the patients' clinical outcomes in terms of survival, treatment responses, and side effects.

DNA *POLD1* was previously found to be altered in 4.47% of melanoma patients (25), but the roles of mutations of *POLD1* in melanoma are not fully understood. However, mutations of *POLD1* were reported to be associated with several other cancer types, including colorectal cancers (26,27). Meanwhile, *ALOX12B* expresses an enzyme which is involved in the conversion of arachidonic acid to 12R-hydroxyeicosatetraenoic acid. A previous study has indicated that overexpression of *ALOX12B* could promote cell proliferation in cervical cancer through regulating PI3K/ERK1 signaling pathway (28). *PTPRT* encodes a member of the protein tyrosine phosphatase (PTP) family. Truncation mutations of *PTPRT* have been associated with metastatic melanomas (29). However, as in *POLD1*, studies have also demonstrated that mutations of *PTPRT* may play crucial roles in other cancers (30), and *PTPRT* may be a potential biomarker for bevacizumab resistance

in colorectal cancers (31). As a member of JAK/STAT pathway (32), recurrent *PTPRT/JAK2* mutations were also found to have a significantly higher prevalence in African Americans lung adenocarcinoma patients (33). Overall, these 3 genes have been linked to oncogenesis or cancer development to some extent. However, none of the 3 genes have been demonstrated to act as a solid survival predictor in melanomas. Our analysis illustrated that patients with these genes' mutation combination had a significantly lower survival rate, suggesting the potential roles of these genes' functions in melanoma progression.

Using machine-learning-based algorithms, we were also able to integrate both the molecular alterations and the clinical outcomes into the analysis. Through combining the clinical data and the NGS panel results, we successfully established models that not only could predict the treatment response but also the side effects of the treatment. Although the oncogenic molecular alterations were particularly good predictors for treatment response, their prediction power was at least better than that of using the clinical features alone. This result indicates that using clinical NGS panels to acquire patients' genetic alterations could significantly improve diagnosis or prediction. Interestingly, we also established a model for predicting the side effect levels from treatment by combining the clinical features and the oncogenic alterations. Surprisingly, our model yielded an AUROC score of 0.8, which indicates this may be a powerful tool for this specific prediction. Taken together, these data suggest that the clinical NGS panel screen could significantly increase the prediction power for the clinical outcome of patients with melanoma.

Conclusions

Precision oncology is an emerging approach for cancer treatment and aims to ensure the treatment is specifically designed and targeted to the unique form of the cancer. Overall, our NGS panel-based study represent a potential genotype guide for patients with melanoma in choosing different therapeutic strategies. Future studies should focus on increasing the sample size for validating our findings. In addition, more mechanistic studies should be focused on how mutations in these genes affect survival, side effects, or treatment response.

Acknowledgments

The authors appreciate the academic support from AME Melanoma Collaborative Group.

Funding: This work was financially supported by the Shanghai Committee of Science and Technology, China (Grant No. 19411951700, to Yong Chen), LinGang Laboratory (Grant No. LG-QS-202205-11, to Wei Sun), and the National Natural Science Foundation of China (Grant Nos. 82272857 and 81802636, to Wei Sun).

Footnote

Data Sharing Statement: Available at <https://atm.amegroups.com/article/view/10.21037/atm-22-5346/dss>

Conflicts of Interest: All authors have completed the ICMJE uniform disclosure form (available at <https://atm.amegroups.com/article/view/10.21037/atm-22-5346/coif>). WS reports funding support from the LinGang Laboratory (Grant No. LG-QS-202205-11), and the National Natural Science Foundation of China (Grant Nos. 82272857 and 81802636). YC reports funding support from the Shanghai Committee of Science and Technology, China (Grant No. 19411951700). JW is from MyGenostics Inc. The other authors have no conflicts of interest to declare.

Ethical Statement: The authors are accountable for all aspects of the work in ensuring that questions related to the accuracy or integrity of any part of the work are appropriately investigated and resolved. The study was conducted in accordance with the Declaration of Helsinki (as revised in 2013). This study was approved by the Medical Ethics Committee of FUSCC (No. 1903198-8) and informed consent was taken from all the patients.

Open Access Statement: This is an Open Access article distributed in accordance with the Creative Commons Attribution-NonCommercial-NoDerivs 4.0 International License (CC BY-NC-ND 4.0), which permits the non-commercial replication and distribution of the article with the strict proviso that no changes or edits are made and the original work is properly cited (including links to both the formal publication through the relevant DOI and the license). See: <https://creativecommons.org/licenses/by-nc-nd/4.0/>.

References

1. Sandru A, Voinea S, Panaitescu E, et al. Survival rates of patients with metastatic malignant melanoma. *J Med Life* 2014;7:572-6.
2. Siegel RL, Miller KD, Jemal A. Cancer statistics, 2020.

- CA Cancer J Clin 2020;70:7-30.
3. Enewold L, Sharon E, Harlan LC. Metastatic Melanoma: Treatment and Survival in the US after the Introduction of Ipilimumab and Vemurafenib. *Oncol Res Treat* 2017;40:174-83.
 4. Schadendorf D, van Akkooi ACJ, Berking C, et al. Melanoma. *Lancet* 2018;392:971-84.
 5. Larkin J, Ascierto PA, Dréno B, et al. Combined vemurafenib and cobimetinib in BRAF-mutated melanoma. *N Engl J Med* 2014;371:1867-76.
 6. Robert C, Karaszewska B, Schachter J, et al. Improved overall survival in melanoma with combined dabrafenib and trametinib. *N Engl J Med* 2015;372:30-9.
 7. Larkin J, Minor D, D'Angelo S, et al. Overall Survival in Patients With Advanced Melanoma Who Received Nivolumab Versus Investigator's Choice Chemotherapy in CheckMate 037: A Randomized, Controlled, Open-Label Phase III Trial. *J Clin Oncol* 2018;36:383-90.
 8. Weber JS, D'Angelo SP, Minor D, et al. Nivolumab versus chemotherapy in patients with advanced melanoma who progressed after anti-CTLA-4 treatment (CheckMate 037): a randomised, controlled, open-label, phase 3 trial. *Lancet Oncol* 2015;16:375-84.
 9. Robert C, Thomas L, Bondarenko I, et al. Ipilimumab plus dacarbazine for previously untreated metastatic melanoma. *N Engl J Med* 2011;364:2517-26.
 10. Ribas A, Kefford R, Marshall MA, et al. Phase III randomized clinical trial comparing tremelimumab with standard-of-care chemotherapy in patients with advanced melanoma. *J Clin Oncol* 2013;31:616-22.
 11. Buchbinder EI, Sosman JA, Lawrence DP, et al. Phase 2 study of sunitinib in patients with metastatic mucosal or acral melanoma. *Cancer* 2015;121:4007-15.
 12. Guo J, Si L, Kong Y, et al. Phase II, open-label, single-arm trial of imatinib mesylate in patients with metastatic melanoma harboring c-Kit mutation or amplification. *J Clin Oncol* 2011;29:2904-9.
 13. Hayward NK, Wilmott JS, Waddell N, et al. Whole-genome landscapes of major melanoma subtypes. *Nature* 2017;545:175-80.
 14. Manca A, Paliogiannis P, Colombino M, et al. Mutational concordance between primary and metastatic melanoma: a next-generation sequencing approach. *J Transl Med* 2019;17:289.
 15. Park C, Kim M, Kim MJ, et al. Clinical Application of Next-Generation Sequencing-Based Panel to BRAF Wild-Type Advanced Melanoma Identifies Key Oncogenic Alterations and Therapeutic Strategies. *Mol Cancer Ther* 2020;19:937-44.
 16. Johnson DB, Frampton GM, Rioth MJ, et al. Targeted Next Generation Sequencing Identifies Markers of Response to PD-1 Blockade. *Cancer Immunol Res* 2016;4:959-67.
 17. Conroy JM, Pabla S, Nesline MK, et al. Next generation sequencing of PD-L1 for predicting response to immune checkpoint inhibitors. *J Immunother Cancer* 2019;7:18.
 18. Lokhandwala PM, Tseng LH, Rodriguez E, et al. Clinical mutational profiling and categorization of BRAF mutations in melanomas using next generation sequencing. *BMC Cancer* 2019;19:665.
 19. Gershenwald JE, Scolyer RA. Melanoma Staging: American Joint Committee on Cancer (AJCC) 8th Edition and Beyond. *Ann Surg Oncol* 2018;25:2105-10.
 20. Chalmers ZR, Connelly CF, Fabrizio D, et al. Analysis of 100,000 human cancer genomes reveals the landscape of tumor mutational burden. *Genome Med* 2017;9:34.
 21. Berland L, Heeke S, Humbert O, et al. Current views on tumor mutational burden in patients with non-small cell lung cancer treated by immune checkpoint inhibitors. *J Thorac Dis* 2019;11:S71-80.
 22. Wang F, Zhao Q, Wang YN, et al. Evaluation of POLE and POLD1 Mutations as Biomarkers for Immunotherapy Outcomes Across Multiple Cancer Types. *JAMA Oncol* 2019;5:1504-6.
 23. Mao L, Qi Z, Zhang L, et al. Immunotherapy in Acral and Mucosal Melanoma: Current Status and Future Directions. *Front Immunol* 2021;12:680407.
 24. Zheng Q, Li J, Zhang H, et al. Immune Checkpoint Inhibitors in Advanced Acral Melanoma: A Systematic Review. *Front Oncol* 2020;10:602705.
 25. AACR Project GENIE Consortium. AACR Project GENIE: Powering Precision Medicine through an International Consortium. *Cancer Discov* 2017;7:818-31.
 26. Bellido F, Pineda M, Aiza G, et al. POLE and POLD1 mutations in 529 kindred with familial colorectal cancer and/or polyposis: review of reported cases and recommendations for genetic testing and surveillance. *Genet Med* 2016;18:325-32.
 27. Buchanan DD, Stewart JR, Clendenning M, et al. Risk of colorectal cancer for carriers of a germ-line mutation in POLE or POLD1. *Genet Med* 2018;20:890-5.
 28. Jiang T, Zhou B, Li YM, et al. ALOX12B promotes carcinogenesis in cervical cancer by regulating the PI3K/ERK1 signaling pathway. *Oncol Lett* 2020;20:1360-8.
 29. Ding L, Kim M, Kanchi KL, et al. Clonal architectures and driver mutations in metastatic melanomas. *PLoS One* 2014;9:e111153.

30. Lee JW, Jeong EG, Lee SH, et al. Mutational analysis of PTPRT phosphatase domains in common human cancers. *APMIS* 2007;115:47-51.
31. Hsu HC, Lapke N, Chen SJ, et al. PTPRT and PTPRD Deleterious Mutations and Deletion Predict Bevacizumab Resistance in Metastatic Colorectal Cancer Patients. *Cancers (Basel)* 2018;10:314.
32. Peyser ND, Freilino M, Wang L, et al. Frequent promoter hypermethylation of PTPRT increases STAT3 activation and sensitivity to STAT3 inhibition in head and neck cancer. *Oncogene* 2016;35:1163-9.
33. Mitchell KA, Nichols N, Tang W, et al. Recurrent PTPRT/JAK2 mutations in lung adenocarcinoma among African Americans. *Nat Commun* 2019;10:5735.

Cite this article as: Sun W, Zhao F, Hu T, Wu Z, Xu Y, Dong Y, Zheng B, Wang C, Yan W, Zhu X, Wu J, McKay MJ, Arozarena I, Alos L, Teixido C, Chen Y. Oncogenic alterations reveal key strategies for precision oncology in melanoma treatment. *Ann Transl Med* 2022;10(22):1246. doi: 10.21037/atm-22-5346

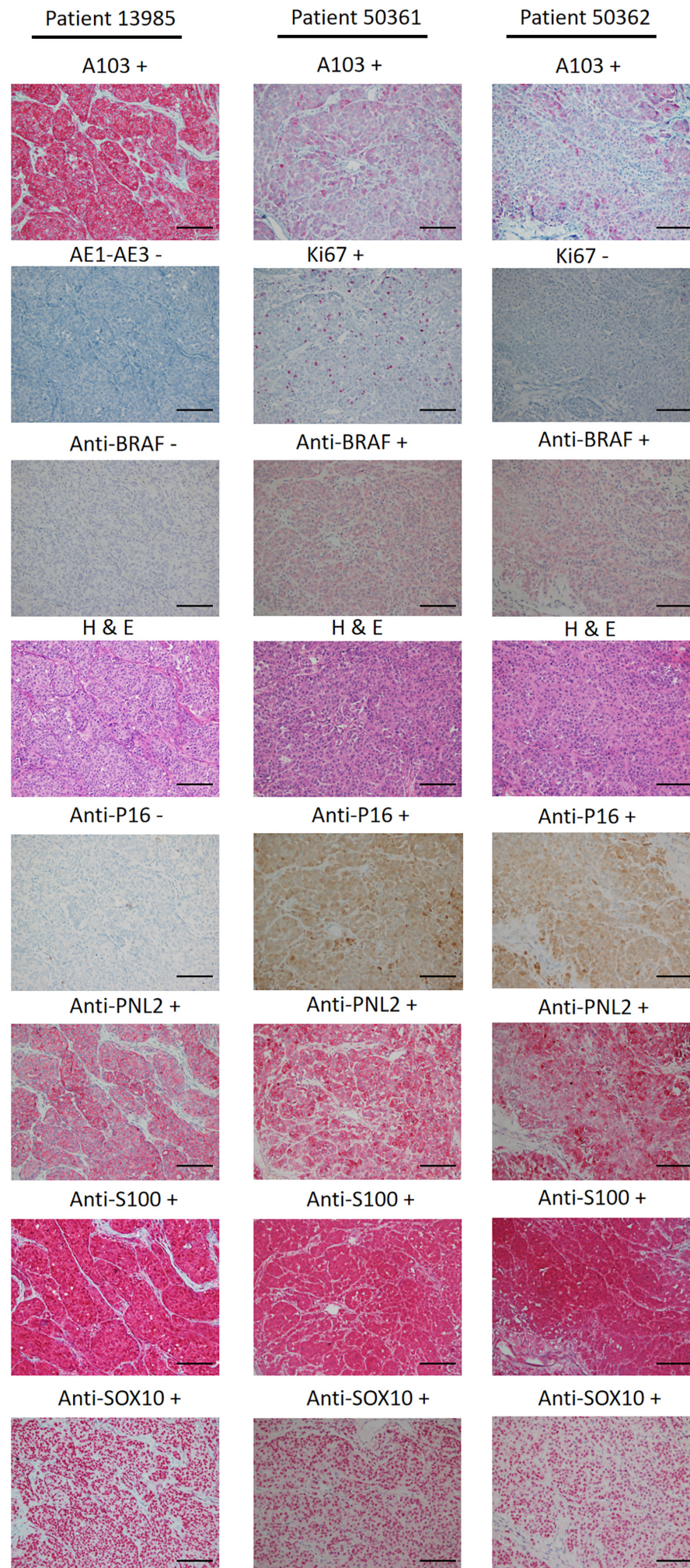


Figure S1 Example immunohistochemical staining slides of melanoma from three patients (scale bar: 100 μ m). H&E, hematoxylin and eosin.

Table S1 Five hundred and fifty-nine tumor-related genes

| | | | | | | | | | | | | | |
|-----------------|-----------------|-----------------|-----------------|-----------------|-----------------|-----------------|------------------|-----------------|-----------------|-----------------|-----------------|-----------------|-----------------|
| <i>ABL1</i> | <i>ABL2</i> | <i>ABRAXAS1</i> | <i>ACVR1</i> | <i>ACVR1B</i> | <i>ADGRA2</i> | <i>AGO2</i> | <i>AKT1</i> | <i>AKT2</i> | <i>AKT3</i> | <i>ALK</i> | <i>ALOX12B</i> | <i>AMER1</i> | <i>ANKRD11</i> |
| <i>APC</i> | <i>AR</i> | <i>ARAF</i> | <i>ARFRP1</i> | <i>ARID1A</i> | <i>ARID1B</i> | <i>ARID2</i> | <i>ARID5B</i> | <i>ASXL1</i> | <i>ASXL2</i> | <i>ATM</i> | <i>ATR</i> | <i>ATRX</i> | <i>AURKA</i> |
| <i>AURKB</i> | <i>AXIN1</i> | <i>AXIN2</i> | <i>AXL</i> | <i>B2M</i> | <i>BABAM1</i> | <i>BAP1</i> | <i>BARD1</i> | <i>BBC3</i> | <i>BCL10</i> | <i>BCL2</i> | <i>BCL2L1</i> | <i>BCL2L11</i> | <i>BCL2L2</i> |
| <i>BCL6</i> | <i>BCOR</i> | <i>BCORL1</i> | <i>BCR</i> | <i>BIRC3</i> | <i>BLM</i> | <i>BMPR1A</i> | <i>BRAF</i> | <i>BRCA1</i> | <i>BRCA2</i> | <i>BRD4</i> | <i>BRIP1</i> | <i>BTG1</i> | <i>BTG2</i> |
| <i>BTK</i> | <i>CALR</i> | <i>CARD11</i> | <i>CARM1</i> | <i>CASP8</i> | <i>CBFB</i> | <i>CBL</i> | <i>CCND1</i> | <i>CCND2</i> | <i>CCND3</i> | <i>CCNE1</i> | <i>CCNQ</i> | <i>CD22</i> | <i>CD274</i> |
| <i>CD276</i> | <i>CD70</i> | <i>CD74</i> | <i>CD79A</i> | <i>CD79B</i> | <i>CDC42</i> | <i>CDC73</i> | <i>CDH1</i> | <i>CDK12</i> | <i>CDK4</i> | <i>CDK6</i> | <i>CDK8</i> | <i>CDKN1A</i> | <i>CDKN1B</i> |
| <i>CDKN2A</i> | <i>CDKN2B</i> | <i>CDKN2C</i> | <i>CEBPA</i> | <i>CENPA</i> | <i>CHD2</i> | <i>CHD4</i> | <i>CHEK1</i> | <i>CHEK2</i> | <i>CIC</i> | <i>CREBBP</i> | <i>CRKL</i> | <i>CRLF2</i> | <i>CSDE1</i> |
| <i>CSF1R</i> | <i>CSF3R</i> | <i>CTCF</i> | <i>CTLA4</i> | <i>CTNNA1</i> | <i>CTNNB1</i> | <i>CUL3</i> | <i>CUL4A</i> | <i>CXCR4</i> | <i>CYLD</i> | <i>CYP17A1</i> | <i>CYSLTR2</i> | <i>DAXX</i> | <i>DCUN1D1</i> |
| <i>DDR1</i> | <i>DDR2</i> | <i>DICER1</i> | <i>DIS3</i> | <i>DNAJB1</i> | <i>DNMT1</i> | <i>DNMT3A</i> | <i>DNMT3B</i> | <i>DOT1L</i> | <i>DROSHA</i> | <i>DUSP4</i> | <i>E2F3</i> | <i>EED</i> | <i>EGFL7</i> |
| <i>EGFR</i> | <i>EIF1AX</i> | <i>EIF4A2</i> | <i>EIF4E</i> | <i>ELF3</i> | <i>ELOC</i> | <i>EMSY</i> | <i>EP300</i> | <i>EPAS1</i> | <i>EPCAM</i> | <i>EPHA3</i> | <i>EPHA5</i> | <i>EPHA7</i> | <i>KMT5A</i> |
| <i>KNSTRN</i> | <i>KRAS</i> | <i>LATS1</i> | <i>LATS2</i> | <i>LMO1</i> | <i>LRP1B</i> | <i>LTK</i> | <i>LYN</i> | <i>LZTR1</i> | <i>MAF</i> | <i>MAGI2</i> | <i>MALT1</i> | <i>MAP2K1</i> | <i>MAP2K2</i> |
| <i>MAP2K4</i> | <i>MAP3K1</i> | <i>MAP3K13</i> | <i>MAP3K14</i> | <i>MAPK1</i> | <i>MAPK3</i> | <i>MAPKAP1</i> | <i>MAX</i> | <i>MCL1</i> | <i>MDC1</i> | <i>MDM2</i> | <i>MDM4</i> | <i>MED12</i> | <i>MEF2B</i> |
| <i>MEN1</i> | <i>MERTK</i> | <i>MET</i> | <i>MGA</i> | <i>MITF</i> | <i>MKNK1</i> | <i>MLH1</i> | <i>MPL</i> | <i>MRE11</i> | <i>MSH2</i> | <i>MSH3</i> | <i>MSH6</i> | <i>MSI1</i> | <i>MSI2</i> |
| <i>MST1</i> | <i>MST1R</i> | <i>MTAP</i> | <i>MTOR</i> | <i>MUTYH</i> | <i>MYB</i> | <i>MYC</i> | <i>MYCL</i> | <i>MYCN</i> | <i>MYD88</i> | <i>MYOD1</i> | <i>NBN</i> | <i>NCOA3</i> | <i>NCOR1</i> |
| <i>NEGR1</i> | <i>NF1</i> | <i>NF2</i> | <i>NFE2L2</i> | <i>NFKBIA</i> | <i>NKX2-1</i> | <i>NKX3-1</i> | <i>NOTCH1</i> | <i>NOTCH2</i> | <i>NOTCH3</i> | <i>NOTCH4</i> | <i>NPM1</i> | <i>NRAS</i> | <i>NSD1</i> |
| <i>NSD2</i> | <i>NSD3</i> | <i>NT5C2</i> | <i>NTHL1</i> | <i>NTRK1</i> | <i>NTRK2</i> | <i>NTRK3</i> | <i>NUF2</i> | <i>NUP93</i> | <i>NUTM1</i> | <i>P2RY8</i> | <i>PAK1</i> | <i>PAK3</i> | <i>PAK5</i> |
| <i>PALB2</i> | <i>PARP1</i> | <i>PARP2</i> | <i>PARP3</i> | <i>PAX5</i> | <i>PAX8</i> | <i>PBRM1</i> | <i>PDCD1</i> | <i>PDCD1LG2</i> | <i>PDGFRA</i> | <i>PDGFRB</i> | <i>PDK1</i> | <i>PDPK1</i> | <i>PGR</i> |
| <i>PHOX2B</i> | <i>PIK3C2B</i> | <i>PIK3C2G</i> | <i>PIK3C3</i> | <i>PIK3CA</i> | <i>PIK3CB</i> | <i>PIK3CD</i> | <i>PIK3CG</i> | <i>PIK3R1</i> | <i>PIK3R2</i> | <i>PIK3R3</i> | <i>PIM1</i> | <i>PLCG2</i> | <i>PLK2</i> |
| <i>PMAIP1</i> | <i>PMS1</i> | <i>PMS2</i> | <i>PNRC1</i> | <i>POLD1</i> | <i>POLE</i> | <i>PPARG</i> | <i>PPM1D</i> | <i>PPP2R1A</i> | <i>PPP2R2A</i> | <i>PPP4R2</i> | <i>PPP6C</i> | <i>PRDM1</i> | <i>PRDM14</i> |
| <i>PREX2</i> | <i>PRKAR1A</i> | <i>PRKCI</i> | <i>PRKD1</i> | <i>PRKDC</i> | <i>PRKN</i> | <i>PRSS8</i> | <i>PTCH1</i> | <i>PTEN</i> | <i>PTP4A1</i> | <i>PTPN11</i> | <i>PTPRD</i> | <i>EPHB1</i> | <i>EPHB4</i> |
| <i>ERBB2</i> | <i>ERBB3</i> | <i>ERBB4</i> | <i>ERCC2</i> | <i>ERCC3</i> | <i>ERCC4</i> | <i>ERCC5</i> | <i>ERF</i> | <i>ERG</i> | <i>ERRFI1</i> | <i>ESR1</i> | <i>ETV1</i> | <i>ETV4</i> | <i>ETV5</i> |
| <i>ETV6</i> | <i>EWSR1</i> | <i>EZH1</i> | <i>EZH2</i> | <i>EZR</i> | <i>FAM46C</i> | <i>FANCA</i> | <i>FANCC</i> | <i>FANCD2</i> | <i>FANCE</i> | <i>FANCF</i> | <i>FANCG</i> | <i>FANCL</i> | <i>FAS</i> |
| <i>FAT1</i> | <i>FBXW7</i> | <i>FGF10</i> | <i>FGF12</i> | <i>FGF14</i> | <i>FGF19</i> | <i>FGF23</i> | <i>FGF3</i> | <i>FGF4</i> | <i>FGF6</i> | <i>FGFR1</i> | <i>FGFR2</i> | <i>FGFR3</i> | <i>FGFR4</i> |
| <i>FH</i> | <i>FLCN</i> | <i>FLT1</i> | <i>FLT3</i> | <i>FLT4</i> | <i>FOXA1</i> | <i>FOXL2</i> | <i>FOXO1</i> | <i>FOXP1</i> | <i>FRS2</i> | <i>FUBP1</i> | <i>FYN</i> | <i>GABRA6</i> | <i>GATA1</i> |
| <i>GATA2</i> | <i>GATA3</i> | <i>GATA4</i> | <i>GATA6</i> | <i>GID4</i> | <i>GLI1</i> | <i>GNA11</i> | <i>GNA13</i> | <i>GNAQ</i> | <i>GNAS</i> | <i>GPS2</i> | <i>GREM1</i> | <i>GRIN2A</i> | <i>GRM3</i> |
| <i>GSK3B</i> | <i>H3F3A</i> | <i>H3F3B</i> | <i>H3F3C</i> | <i>HDAC1</i> | <i>HGF</i> | <i>HIST1H1C</i> | <i>HIST1H2BD</i> | <i>HIST1H3A</i> | <i>HIST1H3B</i> | <i>HIST1H3C</i> | <i>HIST1H3D</i> | <i>HIST1H3E</i> | <i>HIST1H3F</i> |
| <i>HIST1H3G</i> | <i>HIST1H3H</i> | <i>HIST1H3I</i> | <i>HIST1H3J</i> | <i>HIST2H3C</i> | <i>HIST2H3D</i> | <i>HIST3H3</i> | <i>HLA-A</i> | <i>HLA-B</i> | <i>HNF1A</i> | <i>HOXB13</i> | <i>HRAS</i> | <i>HSD3B1</i> | <i>HSP90AA1</i> |
| <i>ICOSLG</i> | <i>ID3</i> | <i>IDH1</i> | <i>IDH2</i> | <i>IFNGR1</i> | <i>IGF1</i> | <i>IGF1R</i> | <i>IGF2</i> | <i>IKBKE</i> | <i>IKZF1</i> | <i>IL10</i> | <i>IL7R</i> | <i>INHA</i> | <i>INHBA</i> |
| <i>INPP4A</i> | <i>INPP4B</i> | <i>INPPL1</i> | <i>INSR</i> | <i>IRF2</i> | <i>IRF4</i> | <i>IRS1</i> | <i>IRS2</i> | <i>JAK1</i> | <i>JAK2</i> | <i>JAK3</i> | <i>JUN</i> | <i>KAT6A</i> | <i>KDM5A</i> |
| <i>KDM5C</i> | <i>KDM6A</i> | <i>KDR</i> | <i>KEAP1</i> | <i>KEL</i> | <i>KIT</i> | <i>KLF4</i> | <i>KLHL6</i> | <i>KMT2A</i> | <i>KMT2B</i> | <i>KMT2C</i> | <i>KMT2D</i> | <i>PTPRO</i> | <i>PTPRS</i> |
| <i>PTPRT</i> | <i>QKI</i> | <i>RAB35</i> | <i>RAC1</i> | <i>RAC2</i> | <i>RAD21</i> | <i>RAD50</i> | <i>RAD51</i> | <i>RAD51B</i> | <i>RAD51C</i> | <i>RAD51D</i> | <i>RAD52</i> | <i>RAD54L</i> | <i>RAF1</i> |
| <i>RANBP2</i> | <i>RARA</i> | <i>RASA1</i> | <i>RB1</i> | <i>RBM10</i> | <i>RECQL</i> | <i>RECQL4</i> | <i>REL</i> | <i>RET</i> | <i>RFWD2</i> | <i>RHEB</i> | <i>RHOA</i> | <i>RICTOR</i> | <i>RIT1</i> |
| <i>RNF43</i> | <i>ROS1</i> | <i>RPS6KA4</i> | <i>RPS6KB2</i> | <i>RPTOR</i> | <i>RRAGC</i> | <i>RRAS</i> | <i>RRAS2</i> | <i>RSPO2</i> | <i>RTEL1</i> | <i>RUNX1</i> | <i>RUNX1T1</i> | <i>RXRA</i> | <i>RYBP</i> |
| <i>SDC4</i> | <i>SDHA</i> | <i>SDHAF2</i> | <i>SDHB</i> | <i>SDHC</i> | <i>SDHD</i> | <i>SESN1</i> | <i>SESN2</i> | <i>SESN3</i> | <i>SETD2</i> | <i>SF3B1</i> | <i>SGK1</i> | <i>SH2B3</i> | <i>SH2D1A</i> |
| <i>SHOC2</i> | <i>SHQ1</i> | <i>SLC34A2</i> | <i>SLIT2</i> | <i>SLX4</i> | <i>SMAD2</i> | <i>SMAD3</i> | <i>SMAD4</i> | <i>SMARCA4</i> | <i>SMARCB1</i> | <i>SMARCD1</i> | <i>SMO</i> | <i>SMYD3</i> | <i>SNCAIP</i> |
| <i>SOCS1</i> | <i>SOS1</i> | <i>SOX10</i> | <i>SOX17</i> | <i>SOX2</i> | <i>SOX9</i> | <i>SPEN</i> | <i>SPOP</i> | <i>SPRED1</i> | <i>SPTA1</i> | <i>SRC</i> | <i>SRSF2</i> | <i>STAG2</i> | <i>STAT3</i> |
| <i>STAT4</i> | <i>STAT5A</i> | <i>STAT5B</i> | <i>STK11</i> | <i>STK19</i> | <i>STK40</i> | <i>SUFU</i> | <i>SUZ12</i> | <i>SYK</i> | <i>TAF1</i> | <i>TAP1</i> | <i>TAP2</i> | <i>TBX3</i> | <i>TCF3</i> |
| <i>TCF7L2</i> | <i>TEK</i> | <i>TERC</i> | <i>TERT</i> | <i>TET1</i> | <i>TET2</i> | <i>TGFBR1</i> | <i>TGFBR2</i> | <i>TIPARP</i> | <i>TMEM127</i> | <i>TMPRSS2</i> | <i>TNFAIP3</i> | <i>TNFRSF14</i> | <i>TOP1</i> |
| <i>TOP2A</i> | <i>TP53</i> | <i>TP53BP1</i> | <i>TP63</i> | <i>TRAF2</i> | <i>TRAF7</i> | <i>TSC1</i> | <i>TSC2</i> | <i>TSHR</i> | <i>TYRO3</i> | <i>U2AF1</i> | <i>UPF1</i> | <i>VEGFA</i> | <i>VHL</i> |
| <i>VTCN1</i> | <i>WISP3</i> | <i>WT1</i> | <i>WWTR1</i> | <i>XIAP</i> | <i>XPO1</i> | <i>XRCC2</i> | <i>YAP1</i> | <i>YES1</i> | <i>ZBTB2</i> | <i>ZFH3</i> | <i>ZNF217</i> | <i>ZNF703</i> | |
| <i>ABCC1</i> | <i>ABCC2</i> | <i>ABCC4</i> | <i>ABCG2</i> | <i>CCND1</i> | <i>CD3EAP</i> | <i>COMT</i> | <i>CSDE1</i> | <i>CTNNB1</i> | <i>CYP2B6</i> | <i>CYP2C19</i> | <i>CYP2C8</i> | <i>CYP2D6</i> | <i>CYP3A4</i> |
| <i>CYP3A5</i> | <i>DPYD</i> | <i>ERCC1</i> | <i>ERCC2</i> | <i>ESR1</i> | <i>ESR2</i> | <i>FCGR3A</i> | <i>FGFR4</i> | <i>GATA3</i> | <i>GGH</i> | <i>GSTM3</i> | <i>GSTP1</i> | <i>LRP2</i> | <i>MTHFR</i> |
| <i>NOS3</i> | <i>PIK3CA</i> | <i>PTEN</i> | <i>PTGS2</i> | <i>SLC19A1</i> | <i>SLC22A2</i> | <i>SLCO1B3</i> | <i>SOD2</i> | <i>TOP1</i> | <i>TP53</i> | <i>TPMT</i> | <i>TYMS</i> | <i>UGT1A1</i> | <i>UGT1A7</i> |
| <i>UMPS</i> | <i>VEGFA</i> | | | | | | | | | | | | |